714 *Inorg. Chem.* **2011**, *50*, 714–716
DOI: 10.1021/ic102017t

Inorganic Chemistry
Communication

HX Addition and Photochemical H_2 Elimination by Ni NHC Complexes

Chang Hoon Lee, Timothy R. Cook, and Daniel G. Nocera*

Department of Chemistry, 6-335, Massachusetts Institute of Technology, 77 Massachusetts Avenue, Cambridge, Massachusetts 02139-4307, United States

Received October 2, 2010

$Ni(H)(X)(IMes)_2$ was prepared by the addition of HX to $Ni(IMes)_2$ (X = Cl, Br; IMes = 1,3-dimesitylimidazol-2-ylidene). $Ni(H)(Cl)(IMes)_2$ (**1**) was isolated from the reaction mixture of $Ni(IMes)_2$ and 2 equiv of 2,6-lutidine·HCl. $Ni(H)(Br)(IMes)_2$ was prepared in a similar way. Although treatment of $Ni(IMes)_2$ with a HCl·dioxane solution gives rise to a mixture of **1**, $NiCl_2(IMes)_2$, and $NiCl(IMes)_2$, **1** was not isolable from the mixture. All three complexes cocrystallized. Photolysis of these nickel hydrides activates their Ni−H bonds by populating Ni−H σ^* orbitals, which results in the formation of H_2. Treatment of **1** with HCl·dioxane gives rise to H_2 and $NiCl_2(IMes)_2$.

In order to meet growing global energy demands in the absence of greenhouse gas emissions, an alternative carbon neutral energy source and a method to generate fuel from it are needed.[1−3] To this end, solar light is particularly desirable as an alternative energy source and hydrogen (H_2) is an attractive fuel medium for its storage. Accordingly, a significant research investment seeks to find efficient methods to photogenerate H_2 from appropriate substrates.[4−10] HX (X = Cl, Br) is a potential source for H_2; it furnishes H_2 upon reduction by electron-rich metals, including reductions that are light-driven, although these photoreactions are typically stoichiometric[11] and most often they are driven by ultraviolet light.[4,12] The photogeneration of H_2 from HX can be catalytic as long as the M−X bonds, which are formed as the photoproduct of H_2 production, can be activated. Although there have been reports of photocatalytic H_2 generation from HX metal complex adducts,[13−15] as well as efficient photogeneration of X_2 from the M−X bonds,[16−21] these photoconversions are mediated by non-earth-abundant second- and third-row transition-metal elements. To this end, it is imperative to begin developing rational H_2 and X_2 photochemistry that is promoted by complexes of first-row metal complexes.[7] We now report the photogeneration of H_2 from nickel(II) hydride complexes bearing N-heterocyclic carbene (NHC) ligands. The addition of HX to a nickel(0) complex furnishes $Ni(H)(X)(IMes)_2$ (IMes = 1,3-dimesitylimidazol-2-ylidene), which readily yields H_2 upon photolysis.

A facile oxidative addition chemistry of substrates such as organic halides and imidazolium salts to nickel(0) of $Ni(NHC)_2$[22−25] inspired us to explore the HX addition chemistry of $Ni(IMes)_2$. Treatment of $Ni(IMes)_2$ with 2 equiv of a 4.0 M HCl·dioxane solution gives rise to $NiCl_2(IMes)_2$ as a major product with concomitant formation of H_2 along with $Ni(H)(Cl)(IMes)_2$ (**1**) and $NiCl(IMes)_2$ (**2**) as minor products. Hydride complex **1** may be obtained as the major product when $Ni(IMes)_2$ is treated only with 1 equiv of HCl. Nevertheless, we were unable to isolate **1** in pure form from this

*To whom correspondence should be addressed. E-mail: nocera@mit.edu.

(1) Nocera, D. G. *Inorg. Chem.* **2009**, *48*, 10001–10007.
(2) Lewis, N. S.; Nocera, D. G. *Proc. Natl. Acad. Sci. U.S.A.* **2006**, *103*, 15729–15735.
(3) Barber, J. *Chem. Soc. Rev.* **2009**, *38*, 185–196.
(4) Esswein, A. J.; Nocera, D. G. *Chem. Rev.* **2007**, *107*, 4022–4047.
(5) Goldsmith, J. I.; Hudson, W. R.; Lowry, M. S.; Anderson, T. H.; Bernhard, S. *J. Am. Chem. Soc.* **2005**, *127*, 7502–7510.
(6) Arachchige, S. M.; Brown, J. R.; Chang, E.; Jain, A.; Zigler, D. F.; Rangan, K.; Brewer, K. J. *Inorg. Chem.* **2009**, *48*, 1989–2000.
(7) Lazarides, T.; McCormick, T.; Du, P.; Luo, G.; Lindley, B.; Eisenberg, R. *J. Am. Chem. Soc.* **2009**, *131*, 9192–9194.
(8) Gartner, F.; Sundararaju, B.; Surkus, A. E.; Boddien, A.; Loges, B.; Junge, H.; Dixneuf, P. H.; Beller, M. *Angew. Chem., Int. Ed.* **2009**, *48*, 9962–9965.
(9) Tschierlei, S.; Karnahl, M.; Presselt, M.; Dietzek, B.; Guthmuller, J.; Gonzalez, L.; Schmitt, M.; Rau, S.; Popp, J. *Angew. Chem., Int. Ed.* **2010**, *49*, 3981–3984.
(10) Lilac, A.; Alivisatos, A. P. *J. Phys. Chem. Lett.* **2010**, *1*, 1051–1054.
(11) Mann, K. R.; Lewis, N. S.; Miskowski, V. M.; Erwin, D. K.; Hammond, G. S.; Gray, H. B. *J. Am. Chem. Soc.* **1977**, *99*, 5525–5526.
(12) Gray, H. B.; Maverick, A. W. *Science* **1981**, *214*, 1201–1205.
(13) Heyduk, A. F.; Nocera, D. G. *Science* **2001**, *293*, 1639–1641.
(14) Odom, A. L.; Heyduk, A. F.; Nocera, D. G. *Inorg. Chim. Acta* **2000**, *297*, 330–337.
(15) Esswein, A. J.; Veige, A. S.; Nocera, D. G. *J. Am. Chem. Soc.* **2005**, *127*, 16641–16651.
(16) Dempsey, J. L.; Essewein, A. J.; Manke, D. R.; Rosenthal, J.; Soper, J. D.; Nocera, D. G. *Inorg. Chem.* **2005**, *44*, 6879–6892.
(17) Cook, T. R.; Esswein, A. J.; Nocera, D. G. *J. Am. Chem. Soc.* **2007**, *129*, 10094–10095.
(18) Cook, T. R.; Surendranath, Y.; Nocera, D. G. *J. Am. Chem. Soc.* **2009**, *131*, 28–29.
(19) Teets, T. T.; Nocera, D. G. *J. Am. Chem. Soc.* **2009**, *131*, 7411–7420.
(20) Teets, T. T.; Lutterman, D. A.; Nocera, D. G. *Inorg. Chem.* **2009**, *49*, 3035–3043.
(21) Trogler, W. C.; Erwin, D. K.; Geoffroy, G. L.; Gray, H. B. *J. Am. Chem. Soc.* **1978**, *100*, 1160–1163.
(22) Mcquinness, D. S.; Cavell, K. J. *Organometallics* **1999**, *18*, 1596–1605.
(23) Clement, N. D.; Cavell, K. J.; Jones, C.; Elsevier, C. J. *Angew. Chem., Int. Ed.* **2004**, *43*, 1277–1279.
(24) Schaub, T.; Backes, M.; Plietzsch, O.; Radius, U. *Dalton Trans.* **2009**, 7071–7079.
(25) Schaub, T.; Backes, M.; Radius, U. *Eur. J. Inorg. Chem.* **2008**, 2680–2690.

 Published on Web 01/12/2011

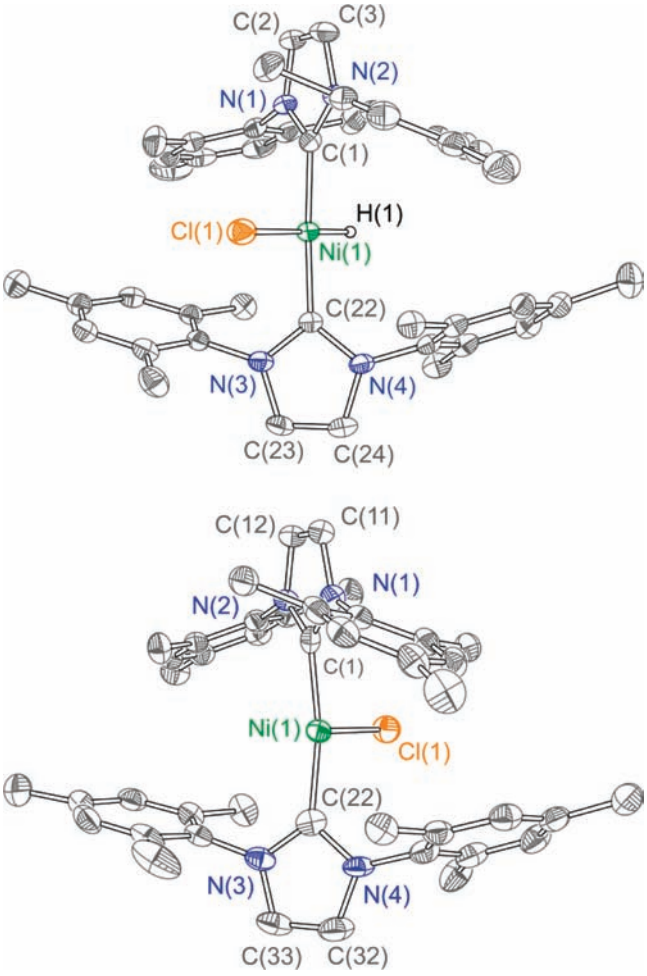

Figure 1. Thermal ellipsoid plots of **1** (top) and **2** (bottom) at the 50% probability level. Hydrogen atoms are omitted for clarity.

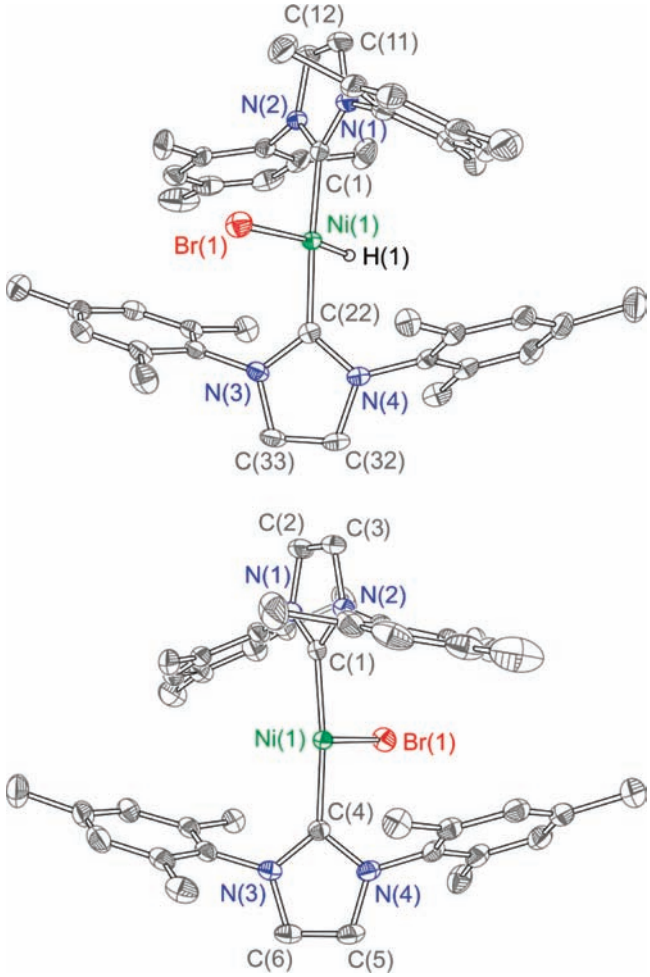

Figure 2. Thermal ellipsoid plots of **3** (top) and **4** (bottom) at the 50% probability level. Hydrogen atoms are omitted for clarity. A bromide from disorder in the crystal is also omitted for clarity.

reaction mixture because of the cocrystallization of $NiCl_2(IMes)_2$ and **2**. **2** was independently obtained from the treatment of $Ni(IMes)_2$ with 4-chlorobenzophenone in analogy to the synthesis of $NiCl(IPr)_2$ using $Ni(IPr)_2$ and aryl chlorides [IPr = 1,3-bis(2,6-diisopropylphenyl)imidazol-2-ylidene].[26] X-ray crystallography confirmed that **2** has a T-shaped geometry about the metal center (Figure 1, bottom).

Treatment of $Ni(IMes)_2$ with 2 equiv of 2,6-lutidine·HCl generates **1** in the absence of **2**.

$$\mathrm{Ni(IMes)_2 + 2Lut\cdot HX \rightarrow Ni(H)(X)(IMes)_2} \quad (\mathrm{X = Cl,\ Br}) \qquad (1)$$

Analytically pure **1** in crystalline form in ca. 70% yield is obtained upon subsequent recrystallization. If the stoichiometry of 2,6-lutidine·HCl is reduced to 1 equiv, in eq 1, **1** is obtained in good yield, but it is accompanied by the formation of $NiCl_2(IMes)_2$ and **2** as minor side products, as determined by NMR. The analogous bromide complex, $Ni(H)(Br)(IMes)_2$ (**3**), also is furnished by the reaction chemistry of eq 1 along with paramagnetic and diamagnetic species that are consistent with $NiBr(IMes)_2$ (**4**) and $NiBr_2(IMes)_2$, respectively. In contrast to **1**, a small amount of $NiBr_2(IMes)_2$, which could not be removed by recrystallization based on NMR analysis and X-ray structure, is obtained when $Ni(IMes)_2$ is treated with 2 equiv of 2,6-lutidine·HBr. However, no **4** is formed.

The crystal structures of **1** and **3**, which are shown in Figures 1 and 2 (top), respectively, reveal a square-planar geometry about the nickel(II) center. The hydride was located crystallographically. The hydride signal appears in the ^{1}H NMR spectrum at −21.9 ppm for **1** and at −20.4 ppm for **3**. The UV−vis absorption spectrum of **1** in toluene is dominated by three features at λ_{max}/nm ($\varepsilon/10^3$ M^{-1} cm^{-1}) = 307 (5.3), 335 (sh, 3.6), and 390 nm (br sh, 0.9). The UV−vis absorption spectrum of **3** is similar to that of **1** (Figure S1 in the Supporting Information), suggesting that the electronic transitions do not possess significant halide character.

Photolysis of **1** and **3** with $\lambda_{exc} > 295$ nm gives rise to H_2 and $NiX(IMes)_2$

$$\mathrm{Ni(H)(X)(IMes)_2} \xrightarrow{\lambda>295\ \mathrm{nm}} \mathrm{Ni(X)(IMes)_2} + \frac{1}{2}\mathrm{H_2} \quad (\mathrm{X = Cl,\ Br}) \qquad (2)$$

at yields of ca. 50% and 70% (X = Cl and Br, respectively) as determined against an internal standard in the ^{1}H NMR spectrum. Intractable side products are formed in small

(26) Miyazaki, S.; Koga, Y.; Matsumoto, T.; Matsubara, K. *Chem. Commun.* **2010**, 1932–1934.

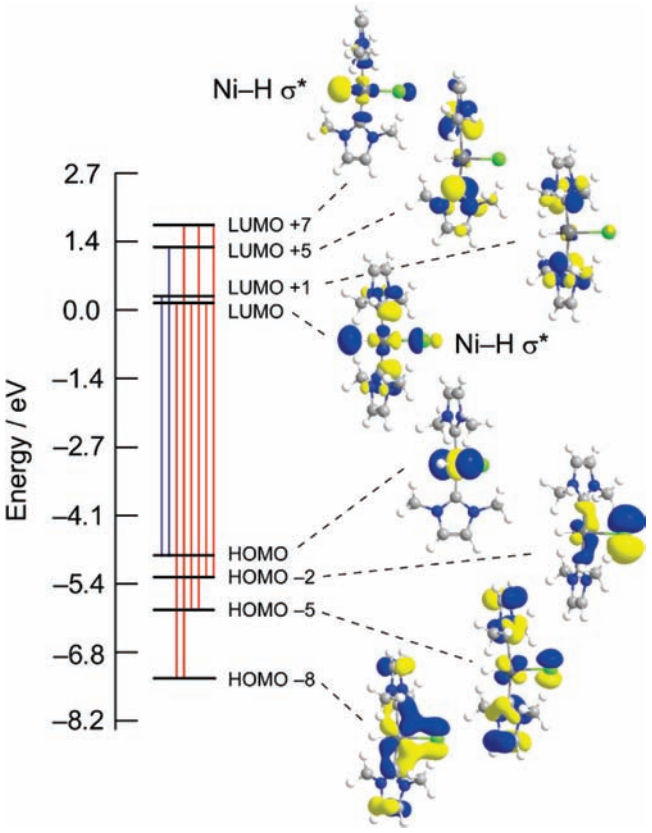

Figure 3. Energy diagram of the orbitals of **1** involved in the most intense electronic transitions above 290 nm. Transitions indicated by blue and red lines correspond to the excitations calculated at 297 nm (blue) and 366 nm (red). The red bars of the molecular orbital picture correspond to the red transition of Figure S1 in the Supporting Information and likewise for blue.

quantities. The single crystal of **4** for X-ray crystallography was obtained from the reaction mixture (Figure 2, bottom). Notably, the yield of H_2 determined by gas chromatography was lower (ca. 33% for X = Cl and 22% for X = Br) than that of $NiX(IMes)_2$, suggesting H_2-consuming side reactions. The presence of these side products hindered kinetic studies to determine quantitatively the rate dependence with respect to the nickel concentration as well as quantum yields. In the case of the latter, the presence of side products caused sufficient perturbation of the absorption spectrum that quantitative assessment of the quantum yields could not be achieved. No further reduction of $NiX(IMes)_2$ was observed under prolonged irradiation. We note that $NiCl_2(IMes)_2$ also does not undergo reduction upon irradiation. The addition of 1 equiv of a HCl·dioxane solution to **1** generates H_2 and $NiCl_2(IMes)_2$ almost quantitatively.

A time-dependent density functional theory calculation of the electronic structure of **1** was performed with the aim of gaining insight into the excited-state parentage from which the photoreactivity of $Ni(H)(X)(IMes)_2$ complexes was derived. Computations were performed on a model complex of **1**, in which the mesityl groups on the nitrogen atoms of the imidazole rings were replaced by methyl groups. The calculated transitions match well the energies and intensities of the observed transitions in the UV−vis spectra of **1** and **3**. Consistent with the observed photochemistry depicted in eq 2, the lowest-energy transitions, which are calculated to have a high oscillator strength, are involved with excited states that arise from the population of orbitals possessing appreciable Ni−H σ^* character (Figure 3). LUMO+7 and LUMO (lowest unoccupied molecular orbital) have hydride character of 4.2% and 4.5%, respectively. Moreover, little halide character is observed in the lowest-energy excited states; the highest contribution of halide character is 10.7% for the LUMO. This result is consistent with the similarity of the absorption spectra of **1** and **3** and the lack of M−X bond activation photochemistry in these complexes. In addition, the excited states have a small but nonnegligible contribution of σ^*(Ni−C) (LUMO+7 and LUMO) and σ^*(Ni−Cl) (LUMO) character. Contributions such as these may explain the formation of side products via excited-state decompositions owing to Ni−ligand bond disruption.

In summary, photolysis of the nickel(II) hydride complexes $Ni(H)(X)(IMes)_2$ gives rise to H_2 with the concomitant formation of the reduced nickel(I) photoproduct $Ni(X)(IMes)_2$. Acid protonolysis of **1** also produces H_2 with the formation of $NiCl_2(IMes)_2$. Calculations reveal that the lowest-energy electronic excitations of **1** and **3** involve population of the Ni−H σ^* orbitals, which is consistent with disruption of the Ni−H bond and observation of H_2 photogeneration.

Acknowledgment. We thank the NSF for support (Grant CHE-0750239). Grants from the NSF also provided instrumental support to the DCIF at MIT (Grants CHE-9808061 and DBI-9729592). We also thank Thomas S. Teets for help with crystallography.

Supporting Information Available: X-ray structural data in CIF format, experimental details, Figure S1 (electronic absorption spectrum and calculated energies and intensities), and X-ray crystal data. This material is available free of charge via the Internet at http://pubs.acs.org.